Improved Oxide Ion Conductivity in $La_{0.8}Sr_{0.2}Ga_{0.8}Mg_{0.2}O_3$ by Doping Co

Tatsumi Ishihara,*,† Haruyoshi Furutani,† Miho Honda,† Takashi Yamada,† Takaaki Shibayama,† Taner Akbay,† Natsuko Sakai,‡ Harumi Yokokawa,‡ and Yusaku Takita†

Department of Applied Chemistry, Faculty of Engineering, Oita University, Dannoharu 700, Oita 870-1192, Japan, and National Institute of Materials and Chemical Research, Tsukuba, Ibaraki, 305-8565, Japan

Received December 28, 1998. Revised Manuscript Received June 7, 1999

The effects of doping Co for the Ga site on the oxide ion conductivity of $La_{0.8}Sr_{0.2}Ga_{0.8}Mg_{0.2}O_3$ have been investigated in detail. It was found that doping Co is effective for enhancing the oxide ion conductivity. In particular, a significant increase in conductivity in the low-temperature range was observed. The electrical conductivity was monotonically increased; however, the transport number for the oxide ion decreased with an increasing amount of Co. Considering the transport number and ion transport number, an optimized amount for the Co doping seems to exist at 8.5 mol % for Ga site. The theoretical electromotive forces were exhibited on H_2-O_2 gas cell utilizing the optimized composition of $La_{0.8}Sr_{0.2}Ga_{0.8}Mg_{0.115}Co_{0.085}O_3$. The diffusion characteristics of the oxide ion in $La_{0.8}Sr_{0.2}Ga_{0.8}Mg_{0.115}Co_{0.085}O_3$ were also investigated by using the ^{18}O tracer method. Since the diffusion coefficient measured by the ^{18}O tracer method was similar to that estimated by the electrical conductivity, the conduction of $La_{0.8}Sr_{0.2}Ga_{0.8}Mg_{0.115}Co_{0.085}O_3$ is concluded to be almost ionic. On the other hand, an oxygen permeation measurement suggests that the oxide ion conductivity increased linearly with an increasing amount of Co. Therefore, specimens with Co content higher than 10 mol % can be considered as a superior mixed oxide ion and hole conductor. The UV−vis spectra suggests that the valence number of doped Co was changed from +3 to +2 with decreasing oxygen partial pressure; the origin of hole conduction can thus be assigned to the formation of Co^{3+}. Since the amount of dopant in the Ga site was compensated with Mg^{2+}, the amount of oxygen deficiency was decreased by doping Co. Therefore, it is likely that the improved oxide ion conductivity observed by doping with Co is brought about by the enhanced mobility of oxide ion.

Introduction

Oxide ion conductors are important functional materials which can be used as electrolytes for fuel cells, oxygen sensors, and films for separating oxygen from air. The development of an oxide ion conductor with a high electrical conductivity has been well-studied.[1] In particular, a fast and stable oxide ion conductor is strongly required for the electrolyte of solid oxide fuel cell (SOFC) to improve the power density and decrease the operating temperature.[2] The fuel cell is considered as the next generation energy production technology as it exhibits clean and highly efficient energy conversion. In particular, the SOFC is important, since the energy conversion efficiency is high and natural gas can be directly used as the fuel.[1] At present, Y_2O_3-stabilized ZrO_2 (YSZ) is widely used as the oxide ion conductor; however, the requirements for excessively high operating temperatures and a thin film are major drawbacks for electrochemical devices utilizing YSZ due to limited oxide ion conductivity.[2] Therefore, the development of an ion conductor with a high electrical conductivity can be regarded as a highly important subject.

A perovskite oxide can accommodate a large amount of vacancies. However, the oxide ion conductivity of these types of oxides has been the subject of a only limited number of investigations.[3−6] Prior to this work, the oxide ion conductivity of perovskite type oxides was investigated, and it was found that $LaGaO_3$ doped with Sr and Mg (LSGM) for the La and Ga sites, respectively, exhibits a higher oxide ion conductivity which is comparable to values reported for CeO_2 doped with Gd.[7,8] The acceptor-doped $LaGaO_3$ is more stable relative to

* Correspondence may be addressed to Dr. Tatsumi Ishihara: Department of Applied Chemistry, Faculty of Engineering, Oita University, Dannoharu 700, Oita 870-1192, Japan. Phone: +81-97-554-7895. Fax: +81-97-554-7979. E-mail: isihara@cc.oita-u.ac.jp.
† Oita University.
‡ National Institute of Materials and Chemical Research.

(1) Choudhary, C. B.; Maiti, H. S.; Subbarao, E. C. *Solid Electrolyte and Their Application*; Subbrao, Ed.; Plenum Press: New York, 1980; p 1.
(2) Minh, N. Q.; Takahashi, T. *Science and Technology of Ceramic Fuel Cells*; Elsevier: New York, 1995.
(3) Takahashi, T.; Iwahara, H. *Energy Convers.* **1972**, *11*, 105.
(4) Kendall, K. R.; Navas, C.; Thomas, J. K.; zur Loye, H.-C. *Solid State Ionics* **1995**, *82*, 215.
(5) Manthiram, A.; Kuo, J. F.; Goodenough, J. B. *Solid State Ionics* **1993**, *62*, 225.
(6) Ishihara, T.; Matsuda, H.; Mizuhara, Y.; Takita, Y. *Solid State Ionics* **1994**, *70/71*, 234.
(7) Ishihara, T.; Matsuda, H.; Takita, Y. *J. Am. Chem. Soc.* **1994**, *116*, 3801.

10.1021/cm981145w CCC: $18.00
Published on Web 07/28/1999

the CeO_2-based material in both reducing and oxidizing atmospheres. Following the authors' first report, a number of investigators have also reported their findings on this system.[9−15] In particular, Baker et al.[9] reported on the ionic conduction of $La_{0.9}Sr_{0.1}GaO_3$ isolated from electron or hole conduction, which in their system, is smaller than the oxide ion conduction by 4 orders of magnitude. They also investigated the effects of Fe and Cr doping for the Ga site of $La_{0.9}Sr_{0.1}GaO_3$. However, doping Fe and Cr decreases the oxide ion conductivity while improving the hole conduction. As in their report, it is generally accepted that doping transition metal cations such as Fe or Co enhances the electron or hole conduction. Therefore, doping these transition metal cations do not seem to be desirable from the oxide ion conduction point of view. On the other hand, a theoretical calculation suggests that oxide ion conductivity of $LaGaO_3$ is further improved by doping Cu^{2+} or Hg^{2+} both of which have lower solution energy than Mg^{2+} on the Ga sublattice.[16] Therefore, it is also possible to get an increased oxide ion conductivity without decreasing the transport number of the ion, provided that the amount of doped transition metal cations is small. From this point of view, the oxide ion conductivity of $LaGaO_3$ doped with Sr for La and Mg and transition metals for the Ga site was investigated,[17] and it was found that doping Co is effective for improving the oxide ion conduction. Since doping Mg for the Ga site seems to be effective in increasing the reactivity of the $LaGaO_3$ oxide, a double-doping strategy for the Ga site has been chosen in this work. A tracer diffusion measurement with ^{18}O is the most effective and reliable method to determine the ionic conductivity.[18] In this study, the oxide ion conductivity of Co-doped La(Sr)-Ga(Mg)O_3 was investigated in detail.

Experimental Section

Sample Preparation. All specimens were prepared by a solid-state reaction using metal oxide powders.[7] Ceramic samples of composition $La_{0.8}Sr_{0.2}Ga_{0.8}$ $Mg_{1-x}Co_xO_3$ were prepared by mixing commercial powders of La_2O_3 (Kishida, 99.99% in pure), $SrCO_3$ (Wako, 99.9%), MgO (Wako, 99.9%), CoO (Rare metal, 99.9%), and Ga_2O_3 (Kishida, 99.99% in pure) in stoichiometric proportions. The starting powders were mixed in an Al_2O_3 pestle and mortar and then precalcined at 1273 K for 6 h. The mixture was pulverized again with a pestle and mortar and pressed into disks of 20 mm in diameter and 1.5 mm in thickness. After isostatic pressing at 275 MPa, the disks were sintered at 1773 K for 6 h in air. The relative densities of the samples used for the conduction measurements ranged from 94 to 98%. For example, the estimated density of $La_{0.8}Sr_{0.2}Ga_{0.8}Mg_{0.115}Co_{0.085}O_3$ was 6.53 g/cm^3 which is 98% of the theoretical density (6.646 g/cm^3). Furthermore, each sample was cut into a rectangular prism (4 × 1 × 15 mm) with a diamond wheel. Platinum paste was applied on both faces of the disks and Pt wires were connected by using a Pt mesh (80 mesh) followed by calcination at 1223 K for 30 min.

The crystal structure of the specimens was determined by X-ray powder diffraction (Rigaku, Rint 2500) with Cu Kα illumination. The lattice parameter was estimated by a least-squares optimization. Magnesium oxide (MgO) at ∼30 vol % was mixed with the specimen as an internal standard. The valence number of Co in the crystal lattice was determined by means of UV−vis spectroscopy. The UV−vis spectra were recorded by the diffuse reflection method (Hitachi, U3410) using an Al_2O_3 disk as a reference. Disk-shaped specimens were preheated at 1223 K for 1 h in H_2, N_2, or O_2 gas flow. The density of the sample was estimated by the Archimedes method.

Electrical Conductivity Measurements. The electrical conductivity of sintered samples were measured as a function of temperature and oxygen partial pressure by a conventional dc four-probe and impedance method in a gas flow system. Each measurement took over an hour at each temperature and oxygen partial pressure to obtain a stable conductivity. It is also noted that the electrical conductivity estimated with the dc four-probe method agrees with that by the impedance method. The partial pressure of oxygen was controlled by mixing N_2, CO, or H_2 with O_2, and the oxygen partial pressure was monitored by an oxygen sensor made of CaO stabilized ZrO_2 that was attached close to the sample. The transport number of the oxide ion was estimated by the electromotive force of the H_2-O_2 gas concentration cell. The oxygen partial pressure was adjusted by adding H_2O to H_2. Here, it seems likely that proton conduction was not observed in the $LaGaO_3$-based oxide, since the conductivity was almost independent of humidity.

Diffusion Measurements. The diffusion profiles of the oxygen was measured by the tracer method utilizing SIMS. Prior to $^{18}O_2$ exchange, the sample was annealed for 1 h in natural oxygen at the same pressure and temperature as the final anneal with ^{18}O. After cooling to room temperature, the sample chamber was evacuated (5×10^{-6} Pa) and labeled oxygen (∼80% enriched $^{18}O_2$) was introduced under a pressure that was the same as for the natural oxygen. The sample was then quickly reheated and annealed for 240 s at 1028 K.

The samples were transversely sectioned and polished as previously described. The diffusion profile of ^{18}O was measured across the polished cross section of the exchanged disk by SIMS line-scanning using a CAMECA IMF-5. An energetic primary ion of 1.1 kV Cs^+ was used, with a current of 1.7 mA, which gives a beam diameter of ∼40 μm. The diffusion and the surface exchange coefficients were determined by fitting the isotopic fraction of oxygen to the solution for the one-dimensional diffusion equation for a semiinfinite media (corrected for the natural isotopic background and normalized to the gas concentration).

An oxygen permeation measurement was also performed to confirm the oxide ion conduction in the specimens. A sintered sample of 17-mm diameter was sealed in Al_2O_3 tubes with molten Pyrex glass. Dry air and nitrogen were introduced to each side of the specimens at 100 mL/min, and the amount of permeated oxygen from air to nitrogen was measured with a TCD gas chromatograph. $La_{0.6}Sr_{0.4}CoO_3$ powder was coated as an electrode on both faces of the cell at 8 mm in diameter followed by calcination at 1225 K for 30 min. The permeation rate was measured as a function of current which was controlled by a Galvanostat (Hioki, HA301).

Results and Discussion

Oxide Ion Conductivity of Co-Doped LSGM. The X-ray diffraction pattern of $La_{0.8}Sr_{0.2}Ga_{0.8}Mg_{0.2-x}Co_xO_3$

(8) Ishihara, T.; Matsuda, H.; Takita, Y. *Solid State Ionics* **1995**, *79*, 147.
(9) Baker, R. T.; Gharbage, B.; Marques, F. M. B. *J. Electrochem. Soc.* **1997**, *144*, 3130.
(10) Drennan, J.; Zelizko, V.; Hay, D.; Ciacchi, F. T.; Rajendran, S.; Badwal, S. P. S. *J. Mater. Chem.* **1997**, *7*, 79.
(11) Feng, M.; Goodenough, J. B. *Eur. J. Solid State Inorg. Chem.* **1994**, *31*, 663.
(12) Huang, P. N.; Petric, A. *J. Electrochem. Soc.* **1996**, *143*, 1644.
(13) Yamaji, K.; Horita, T.; Ishikawa, M.; Sakai, N.; Yokokawa, H. *Solid State Ionics* **1998**, *108*, 415.
(14) Stevenson, J. W.; Armstrong, T. R.; McCready, D. E.; Pederson, L. R.; Weber, W. J. *J. Electrochem. Soc.* **1997**, *144*, 3613.
(15) Huang, K. Q.; Goodenough, J. B. *J. Solid State Chem.* **1998**, *136*, 274.
(16) Khan, M. S.; Islam, M. S.; Bates, D. R. *J. Phys. Chem. B* **1998**, *102*, 3099.
(17) Ishihara, T.; Akbay, T.; Furutani, H.; Nishiguchi, H.; Takita, Y. *Solid State Ionics*, in press.
(18) Ishihara, T.; Kilner, J. A.; Honda, M.; Takita, Y. *J. Am. Chem. Soc.* **1997**, *119*, 2747.

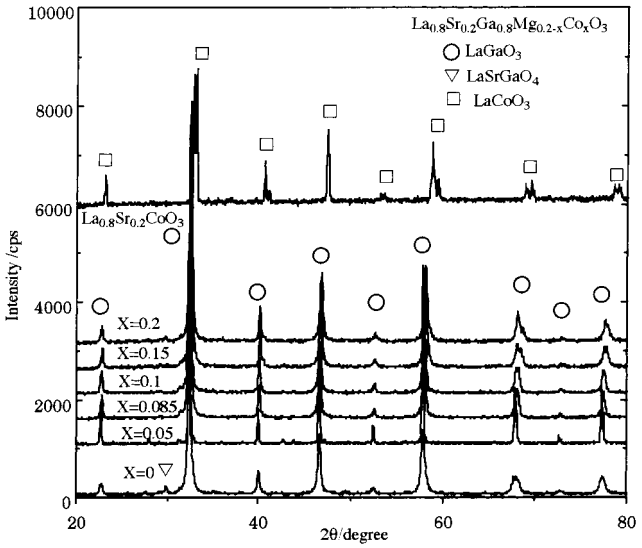

Figure 1. XRD pattern of $La_{0.8}Sr_{0.2}Ga_{0.8}Mg_{0.2-x}Co_xO_3$.

Table 1. Estimated Lattice Parameter and Density of $La_{0.8}Sr_{0.2}Ga_{0.8}Mg_{0.2-x}Co_xO_3$

Co content,	lattice parameter, pm			density, g/cm^3		relative
X	*a*	*b*	*c*	theor	measd	density
0	555.8	553.5	784.5	6.445	6.367	0.988
0.05	555.7	551.5	781.3	6.544	6.361	0.972
0.085	548.5	551.0	779.8	6.683	6.459	0.966
0.10	551.7	552.1	778.9	6.652	6.559	0.986
0.15	554.3	551.7	777.4	6.687	6.633	0.984
0.2	552.0	549.3	777.4	6.735	6.711	0.996
LSG[a]	552.3	553.7	779.7	6.985	–	–

[a] LSG: $La_{0.9}Sr_{0.1}GaO_3$. Relative density = (measured density)/(theoretical density).

is shown in Figure 1. Here, the diffraction patterns of all samples mainly consisted of peaks of the $LaGaO_3$ perovskite phase. Although some peaks at high diffraction angle split at high Co content, all the diffraction peaks were not similar to that of $La_{0.8}Sr_{0.2}CoO_3$, as is shown in Figure 1. Therefore, the formation of $LaCoO_3$-based oxide could not be considered. In addition, the diffraction peaks of $LaGaO_3$ without doping Mg for the Ga site were also split.[8] This suggested that the crystal symmetry is initially not high in the $LaGaO_3$ system. Since no diffraction peaks due to a secondary phase were observed except for $x = 0$ and cobalt has a high solubility in the $LaGaO_3$ lattice, a solid solution of Co into the Ga site in the perovskite lattice was assumed in the composition range examined. It is also noted that the diffraction angle was shifted to a higher angle with increasing Co content, since the ionic size of six-coordinated Co^{3+} is smaller than that of Mg^{2+} and almost the same as that of the six-coordinated Ga^{3+} ion. The higher shift in the diffraction angle also suggested that a solid solution of Co doped at the Ga site in the lattice was performed. Table 1 shows the lattice parameter and density of the specimens as a function of the Co content. The lattice parameter was estimated on the basis of an orthorhombic lattice taken from that of nondoped $LaGaO_3$. It is clearly shown that the lattice parameters b and c decreased with increasing Co content, making it comparable to $LaGaO_3$. On the other hand, the estimated density also monotonically increased with increasing Co concentration. Consequently, it is believed that the doped Co was accommodated at the Ga site in the lattice and made the lattice similar to that of the nondoped one. The relative density of the obtained samples were also noted to be always higher than 0.95% of the theoretical ones.

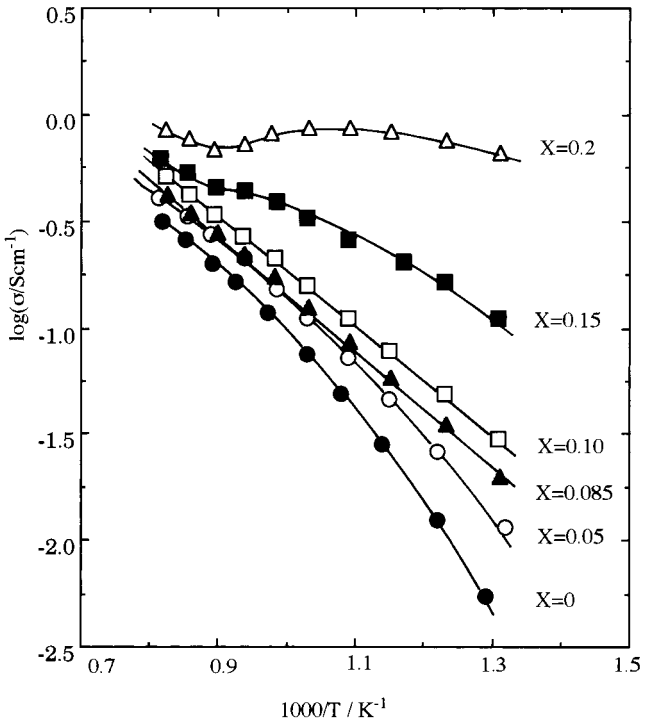

Figure 2. Arrhenius plots of electrical conductivity of $La_{0.8}Sr_{0.2}Ga_{0.8}Mg_{0.2-x}Co_xO_3$.

Figure 2 shows the Arrhenius plots of the electrical conductivity of $La_{0.8}Sr_{0.2}Ga_{0.8}Mg_{0.2-x}Co_xO_3$ in a N_2 flow in which the oxygen partial pressure is 10^{-5} atm. It is obvious that the electrical conductivity of the specimens increased with an increasing amount of doped Co. On the other hand, the slope of the Arrhenius plots was decreased by increasing the amount of Co, suggesting that the activation energy for electrical conduction was decreased. In particular, the electrical conductivity of the specimens at $x = 0.2$ was almost independent of temperature and a significant irregularity was observed at around 1000 K. This suggested that electronic conduction became dominant as the amount of doped Co increased. Figure 3 shows the activation energy for electrical conductivity as a function of the Co concentration. The activation energy was estimated at temperatures above 1000 K. Clearly, the apparent activation energy for electrical conduction monotonically decreases with increasing Co amount and reaches a value of 0.53 eV for 10 mol % Co. The activation energy for electrical conductivity abruptly drops for Co compositions larger than 15 mol %. At $x = 0.2$, the activation energy for electrical conduction was as low as 0.2 eV which strongly suggested that holes became dominant.

To estimate the charge conducting species, the electrical conductivity of the specimens was measured as a function of the oxygen partial pressure and is shown in Figure 4. The electrical conductivity of the specimens with compositions smaller than 10 mol % Co was almost independent of the oxygen partial pressure. On the other hand, the electrical conductivity increases with increasing oxygen partial pressure when the Co concentration is greater than 10 mol %. Therefore, the free

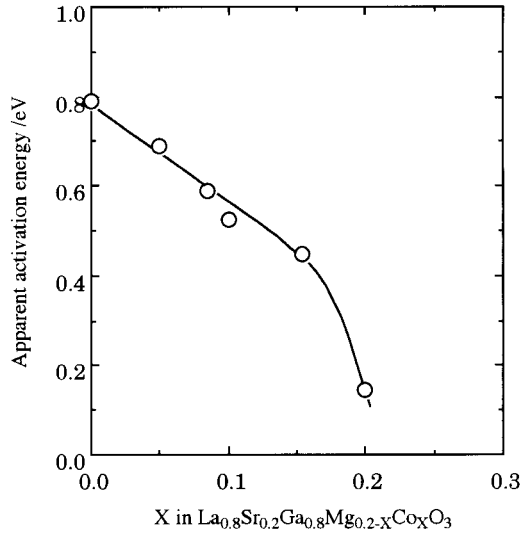

Figure 3. The apparent activation energy for electrical conductivity as a function of x values in $La_{0.8}Sr_{0.2}Ga_{0.8}Mg_{0.2-x}Co_xO_3$.

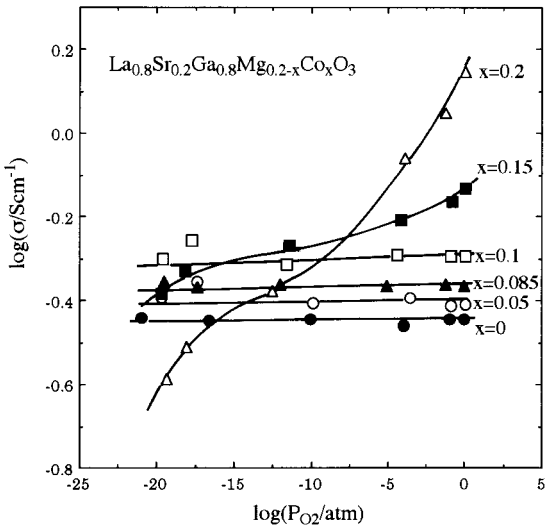

Figure 4. The electrical conductivity of $La_{0.8}Sr_{0.2}Ga_{0.8}Mg_{0.2-x}Co_xO_3$ as a function of oxygen partial pressure.

hole, which may be related to the formation of Co^{3+}, was formed by incorporation of Co into the lattice and the hole conduction becomes more significant with increasing Co concentration. In particular, the electrical conductivity of specimens of $x = 0.2$ monotonically decreased with decreasing oxygen partial pressure within the whole range examined. However, the order of dependence of the electrical conductivity on the oxygen partial pressure for this composition was $\sim 1/50$ which is far smaller than $1/6$ or $1/4$. Therefore, the oxide ion conductivity was still dominant for this composition. Consequently, the increase in the total conductivity shown in Figure 2 is not simply due to the increased ionic conductivity.

The transport number for the oxide ion was estimated with an oxygen concentration cell. Figure 5 shows the temperature dependence of the transport number of the oxide ion. The electromotive forces (emf) almost corresponded to that estimated by the Nernst equation at temperatures higher than 1000 K when the amount of Co is smaller than 10 mol %. On the other hand, the electromotive force became smaller by increasing the Co

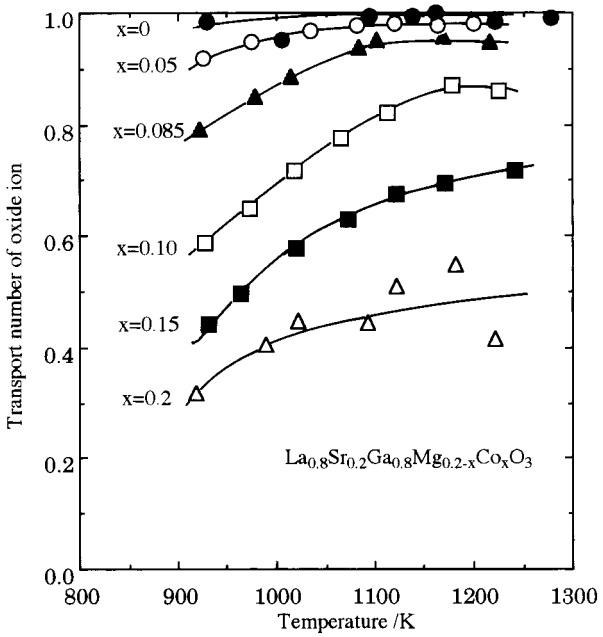

Figure 5. Temperature dependence of the transport number of oxide ion in $La_{0.8}Sr_{0.2}Ga_{0.8}Mg_{0.2-x}Co_xO_3$.

concentration, and it reached almost half of the theoretical value for the specimen with $x = 0.2$. As discussed above, the deviation from the Nernst emf with increasing Co concentration was a result of hole conduction which becomes significant at high oxygen partial pressures. The estimated transport number for the oxide ion decreased with decreasing temperature for all of the samples examined. It is considered that the formation of free holes can be represented by the following defect reaction in the Kröger−Vink notification:

$$^1/_2O_2 + V_O^{\cdot\cdot} = O_O^x + 2h^{\bullet} \qquad (1)$$

This equation means that excess the oxygen is incorporated into the lattice by changing the valence number of Co from +2 to +3 with increasing oxygen partial pressure, since no nonstoichiometry was observed for La^{3+}, Sr^{2+}, Ga^{3+}, and Mg^{2+}. In case of the similar perovskite-type $LaMnO_3$ and $LaCoO_3$ oxide, the amount of excess oxygen increases with decreasing temperature.[19,20] Therefore, it is expected that hole conduction becomes significant with decreasing temperature due to the increased amount of excess lattice oxygen. Consequently, we conclude that the transport number of $LaGaO_3$ doped with Co decreases with decreasing temperature. However, the estimated transport number for the oxide ion is higher than 0.8 at all temperatures when the amount of doped Co was smaller than 0.1. Therefore, the Co-doped $LaGaO_3$-based oxide also serves as a fast oxide ion conductor.

The electrical conductivity shown in Figure 2 is the total conductivity consisting of the hole and oxide ion conduction. To determine the effect of Co on the oxide ion conductivity, the electrical conductivity by holes should be separated from the total conduction. This can be achieved theoretically by multiplying the total con-

(19) Mizusaki, J. *Solid Sate Ionics* **1992**, *52*, 79.
(20) Mizusaki, J.; Tagawa, H.; Naraya, K.; Sasamoto, T. *Solid State Ionics* **1991**, *49*, 111.

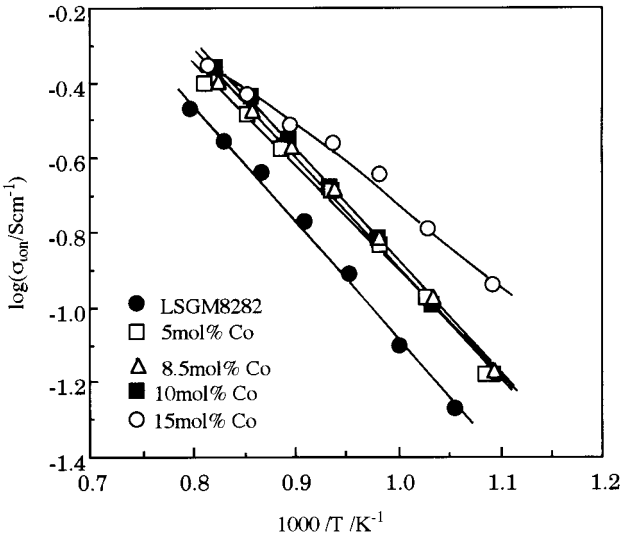

Figure 6. Temperature dependence of the estimated oxide ion conductivity of $La_{0.8}Sr_{0.2}Ga_{0.8}Mg_{0.2-x}Co_xO_3$. Oxide ion conductivity was estimated by total conductivity and transport number.

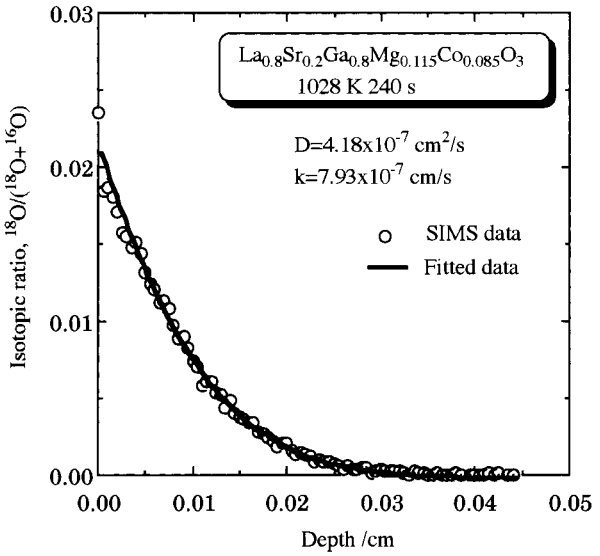

Figure 7. Depth distribution profiles of normalized isotopic fraction for $La_{0.8}Sr_{0.2}Ga_{0.8}Mg_{0.115}Co_{0.085}O_3$ sample showing the experimental and fitted data. Exchange of ^{18}O was performed at 1028 K for 240 s.

ductivity by the estimated transport number using an oxygen concentration cell. However, the transport number of the oxide ion is dependent on the oxygen partial pressure and the estimated transport number obtained from the H_2-O_2 concentration cell is considered as the maximum value within the range of oxygen partial pressures of 1 to 10^{-21} atm. However, as a first approximation, the oxide ion conductivity was estimated by multiplying the total conductivity by the estimated transport number obtained from the oxygen concentration cell. If the estimated transport number of the oxide ion is close to the actual value, then the amount of doped Co was smaller than 10 mol % and the estimated oxide ion conductivity would be also close to the actual value. The temperature dependence of the estimated oxide ion conductivity is shown in Figure 6. The estimated oxide ion conductivity increased with an increasing amount of doped Co and a maximum value is reached at ~10−15 mol % Co.

Although the highest oxide ion conductivity is obtained at around $x = 0.1$, the transport number for the oxide ion is still smaller than 0.9. Therefore, it can be safely concluded that the most promising composition is $La_{0.8}Sr_{0.2}Ga_{0.8}Mg_{0.115}Co_{0.085}O_3$ (denoted as LSGMC). At this composition, the electrical conductivity is almost independent of the oxygen partial pressure from $P_{O_2} = 10^{-21}$ to 1 atm as shown in Figure 3. Therefore, it is expected that the oxide ion conductivity is still dominant and stable over a wide range of oxygen partial pressures. The observed electromotive forces become surprisingly close to the theoretical values as shown in Figure 5; in particular, the ones at temperatures higher than 1073 K show an excellent match. Although the transport number for the oxide ion decreases with a decrease in temperature, it stays higher than 0.8 for the whole temperature range. These results agree with the ones obtained from the oxygen partial pressure dependence of the electrical conductivity. It is also noted that the estimated oxide ion conductivity of LSGMC was ~1.5 times larger than that of LSGM at 1073 K, and the difference became significant with decreasing temperature, since the activation energy for ion conduction of LSGMC and LSGM were 0.55 and 0.79 eV, respectively.

Self-Diffusion of the Oxide Ion in LSGMC. The oxide ion conductivity in LSGMC was further studied by the tracer diffusion method with ^{18}O. The tracer diffusion measurement is the most useful method to determine the transport properties of the oxide ion.[21,22] In a previous study, some of us investigated the diffusion properties of oxygen in LSGM.[18] Figure 7 shows the experimentally determined ^{18}O diffusion profiles in LSGMC, as a result of the isotope exchange at 1028 K for 240 s. The solid line in Figure 7 shows the isotopic fraction calculated from the diffusion equation using the values of D and k fitted to the experimental data. In the case of $LaGaO_3$ doped with Sr and Mg, the surface concentration of ^{18}O at the same temperature is smaller than 0.01, suggesting that LSGM has a limited amount of free electrons. However, the isotopic fraction of ^{18}O at the surface of LSGMC was found to be 0.02, after subtracting the natural background and correcting for the gaseous ^{18}O. This suggests that the surface exchange coefficient is improved by doping Co. In the previous paper, it was pointed out that the rate-determining step for exchange on the surface of YSZ is the charge-transfer process.[18] The improvement in the surface exchange property may be due to the enhanced semiconduction by doping Co. On the other hand, despite the short period and low temperature of ^{18}O exchange, the diffusion depth reached to a value of about 300 μm. This diffusion depth is higher than that of LSGM under the same conditions. Therefore, it is clear that LSGMC exhibits a very high oxide ion diffusion coefficient.

Figure 8 shows the Arrhenius plots of the self-diffusion coefficient and the surface exchange coefficient of oxygen in LSGMC. The diffusion constants were calculated from the estimated oxide ion conductivity data via the Nernst−Einstein relationship and are also

(21) Manning, P. S.; Sirman, J. D.; De Souza, R. A.; Kilner, J. A. *Solid State Ionics* **1997**, *100*, 1.
(22) Steele, B. C. H. *J. Power Source* **1994**, *49*, 1.

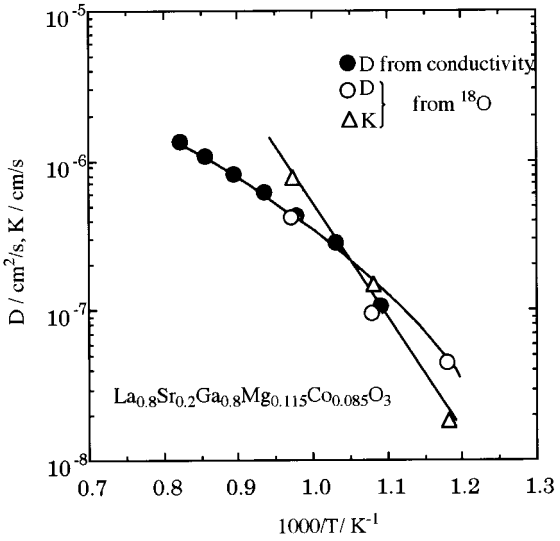

Figure 8. Arrhenius plots of the self-diffusion coefficient and the surface exchange coefficient of oxygen in $La_{0.8}Sr_{0.2}Ga_{0.8}Mg_{0.115}Co_{0.085}O_3$ estimated with ^{18}O trace method.

Table 2. Diffusion Coefficient (*D*) and Surface Exchange Coefficient (*k*) of LSGMC and LSGM at 1028 K

	method	*D*, cm^2/s	k, cm/s
$La_{0.8}Sr_{0.2}Ga_{0.8}Mg_{0.115}Co_{0.085}O_3$ (LSGMC)	SIMS	4.18×10^{-7}	7.93×10^{-7}
	conductivity	4.19×10^{-7}	
$La_{0.8}Sr_{0.2}Ga_{0.8}Mg_{0.2}O_3$ (LSGM)	SIMS	3.74×10^{-7}	3.81×10^{-7}
	conductivity	3.25×10^{-7}	

plotted in Figure 8 for comparison. Table 2 summarizes the estimated diffusion coefficient and surface exchange coefficient obtained by SIMS and conductivity measurements. The measured self-diffusion coefficient of oxide ion agreed with the ones estimated from the electrical conductivity in the measured temperature range. This indicates that the estimated oxide ion conductivity of LSGMC in Figure 7 was very close to the actual value. The activation energy for oxygen self-diffusion of LSGMC was 0.42 eV, which agrees with that from the electrical conductivity. It is also noted that the activation energy of the surface exchange coefficient was 1.54 eV, which is similar to that of LSGM (1.57 eV). The self-diffusion coefficient in LSGMC was ~1.3 times larger than that of LSGM. Therefore, improved oxide ion diffusion property by doping Co is confirmed by ^{18}O diffusion. Consequently, the tracer diffusion measurement also suggested that doping a small amount of Co is effective for increasing the oxide ion conductivity.

Oxygen Permeation Measurement of LSGMC. The oxide ion conductivity in Co-doped $LaGaO_3$ was further measured by the permeation of oxygen to confirm the improved oxide ion conductivity. Figure 9 shows the permeation rate of oxygen in LSGMC and LSGM at 1073 K as a function of current. The amount of oxygen permeation estimated by Faraday's law is also shown by the dotted line. Clearly, the amount of permeated oxygen increased linearly with increasing current for both materials, although oxygen permeation was observed at open circuit in the case of LSGMC. This chemically leaked oxygen under open circuit conditions suggests that a small amount of hole conduction also exists in LSGMC, which also agrees with the results of transport number measurements with gas concentration cells. On the other hand, the amount of permeated

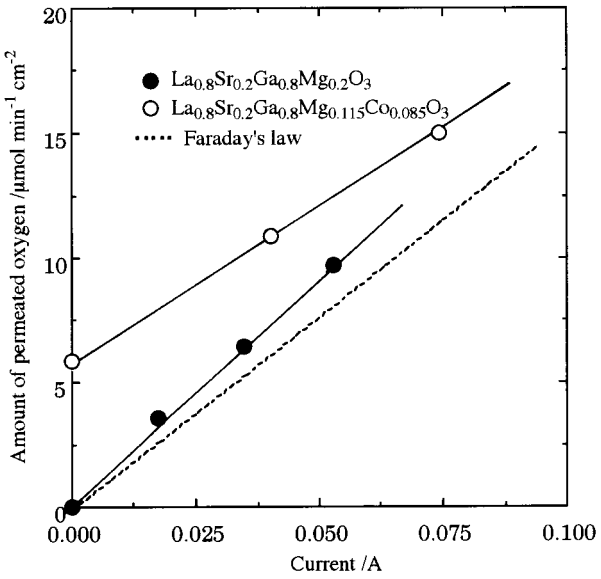

Figure 9. Oxygen permeation rate in $La_{0.8}Sr_{0.2}Ga_{0.8}Mg_{0.115}Co_{0.085}O_3$ and $La_{0.8}Sr_{0.2}Ga_{0.8}Mg_{0.2}O_3$ disk at 1073 K as a function of current.

oxygen was almost the same as that estimated from Faraday's law and furthermore, almost no oxygen flux was observed at open circuit conditions in the case of LSGM. This is due to the wholly ionic conductivity of LSGM. The amount of permeated oxygen in the open and short circuit conditions represents the electronic and the sum of oxide ion and electronic conduction, respectively. In LSGMC under the measurement conditions, the hole is the electronic conducting species, as was discussed previously. By assuming that the hole conduction is independent of the current density, the transport number for the oxide ion (t_{ion}) was theoretically estimated by the following equation:

$$t_{ion} = (F_{O2}{}^{S} - F_{O2}{}^{O})/F_{O2}{}^{S} \quad (2)$$

where $F_{O2}{}^{S}$ and $F_{O2}{}^{O}$ are the amount of oxygen permeated under short circuit and open circuit conditions, respectively. The estimated transport number for LSGMC was ~0.61 which is slightly lower than that of the H_2-O_2 cell. The lower values estimated by oxygen permeation may result from the difference in oxygen partial pressure for the measurements, since the transport number for the oxide ion decreases with increasing oxygen partial pressure due to the significant hole conduction. Furthermore, the overpotential of the electrode also decreased the amount of oxygen under short circuit conditions. It is obvious that the main charge carrier in LSGMC was the oxide ion. On the other hand, the amount of oxygen permeated at open circuit was negligible as in the case of LSGM. This suggested that LSGM is a pure oxide ion conductor. The amount of oxygen permeation of LSGMC at the short circuit was 1.5 times larger than that of LSGM. This agrees with the results of both electrical and isotopic measurements.

Figure 10 shows the temperature dependence of oxygen permeation under short circuit conditions in LSGMC and LSGM. Although the amount of oxygen permeation decreases with decreasing temperature in both specimens, it is obvious that the amount of oxygen permeation is always larger in LSGMC than in LSGM.

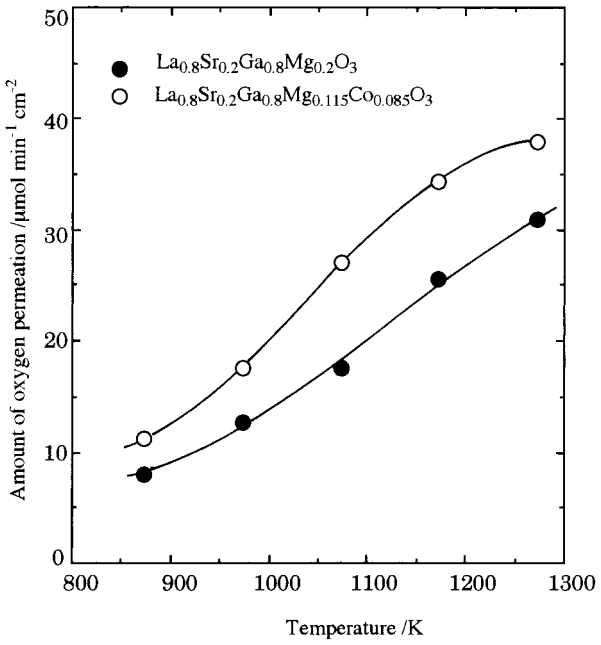

Figure 10. Temperature dependence of oxygen permeation rate at short circuited condition in $La_{0.8}Sr_{0.2}Ga_{0.8}Mg_{0.115}Co_{0.085}O_3$ and $La_{0.8}Sr_{0.2}Ga_{0.8}Mg_{0.2}O_3$.

The difference in the oxygen permeation rate also became significant when the temperature was decreased. The estimated activation energies for oxygen permeation in LSGMC and LSGM were 0.5 and 0.7 eV, respectively. This result also agrees with the electrical conductivity. Thus, it can be concluded that the oxide ion conductivity was improved by partially substituting the Ga site of LSGM with Co, albeit a small amount of hole conduction appears.

Valence Number of Co in the Lattice of $LaGaO_3$. It is well-known that the electrical conductivity is a function of the mobility and carrier concentration. Therefore, to confirm the mechanism of improved oxide ion conductivity by doping Co, determining the valence number of Co in crystal lattice is of great importance. Co^{3+} and Co^{2+} are reported to exhibit strong absorption bands in the UV−vis spectra at different frequencies.[23−26] Therefore, the valence number of doped Co in $LaGaO_3$ lattice was investigated by means of UV−vis spectroscopy. Figure 11 shows the UV−vis spectra of $La_{0.8}Sr_{0.2}Ga_{0.8}Mg_{0.2}O_3$ and $La_{0.8}Sr_{0.2}Ga_{0.8}Mg_{0.115}Co_{0.05}O_3$ after heating at 1173 K for 1 h in O_2, N_2, and H_2 flows. After the heat treatment in O_2 (Figure 11a), two absorption bands were observed at ∼720 and ∼450 nm, which are close to the absorption bands reported for Co^{3+} complexes.[23,24] On the other hand, these absorption bands disappeared and new absorption bands appeared at ∼550 and ∼650 nm after H_2 reduction (Figure 11b and c). Similar UV−vis spectra were also observed for the sample heated in a N_2 atmosphere ($P_{O_2} = \sim 10^{-5}$ atm). The octahedral Co^{2+} complex exhibits similar UV−vis spectra.[25,26] Therefore, the doped Co seems to be divalent at an oxygen partial pressure lower than 10^{-5} atm, and it exists at the six-coordinated site of Ga in the perovskite structure. Sasaki et al. reported that divalent Co is stable in the ZrO_2-based oxide over wide range of oxygen partial pressures.[27] Therefore, it can be said that a large part of the doped Co is divalent over a wide range of oxygen partial pressures and it changes to trivalent cobalt with increasing oxygen partial pressure. As discussed, hole conduction appeared by Co doping in the range of high oxygen partial pressure. The origin of the hole conduction seems to be the formation of Co^{3+}, which is considered as Co^{2+} and a trapped electron hole. Since the amount of dopant in the Ga site was compensated by the amount of Mg, the amount of oxygen vacancies seems to be almost constant in a reducing atmosphere and decreases with increasing oxygen partial pressure when Co^{2+} is changed to Co^{3+}. Consequently, the improved oxide ion conductivity by doping Co seems to be brought about by an improved mobility of the oxide ion within the lattice, since the number of oxygen vacancies is not increased by doping Co. The ionic size of six-coordinated Mg^{2+} (66 pm) is slightly larger than that of Ga^{3+} (62 pm). Therefore, the local stress in the lattice due to the mismatch in ionic size of Mg^{2+} and Ga^{3+} seems to decrease the mobility of the oxide ion. On the other hand, the ionic radius of the six-coordinated Co^{3+} (63 pm) is almost the same as that of

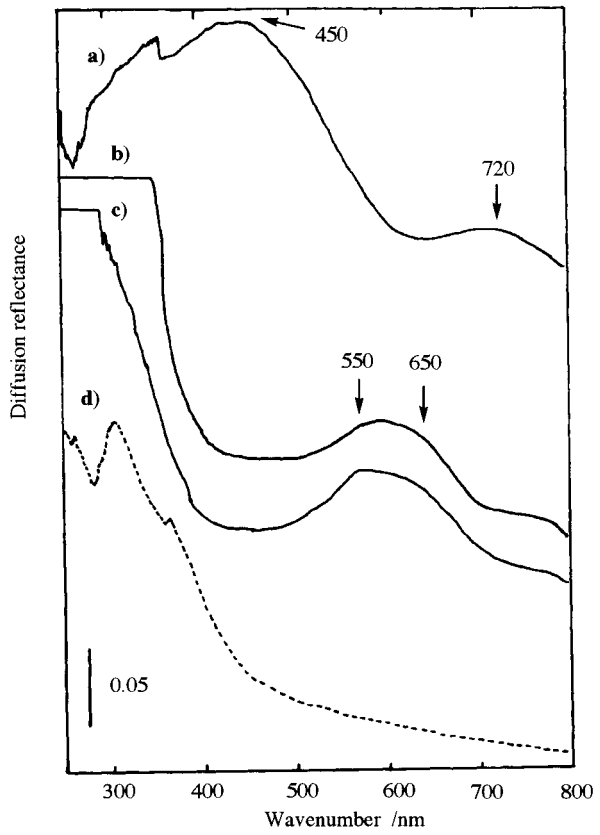

Figure 11. UV−vis spectra of $La_{0.8}Sr_{0.2}Ga_{0.8}Mg_{0.15}Co_{0.05}O_3$ and $La_{0.8}Sr_{0.2}Ga_{0.8}Mg_{0.2}O_3$ after calcination at 1223 K for 1 h in H_2, N_2, and O_2 flow: $La_{0.8}Sr_{0.2}Ga_{0.8}Mg_{0.115}Co_{0.085}O_3$, (a) O_2, (b) N_2, (c) H_2; and $La_{0.8}Sr_{0.2}Ga_{0.8}Mg_{0.2}O_3$, (d) H_2.

(23) Cotton, F. A.; Wilkinson, G. *Advanced Inorganic Chemistry*, 5th ed.; John Wiley & Sons: New York, 1988; p 731.
(24) Baker, L. C.; Simmons, V. W. *J. Am. Chem. Soc.* **1959**, *81*, 4744.
(25) Cotton, F. A.; Wilkinson, G. *Advanced Inorganic Chemistry*, 5th ed.; John Wiley & Sons: New York, 1988; p 734.
(26) Kurshev, V.; Kevan, L.; Parillo, D. J.; Pereira, C.; Kokotailo, G. T.; Gorte, R. J. *J. Phys. Chem.* **1994**, *98*, 10160.
(27) Sasaki, K.; Murugaraj, P.; Haseidl, M.; Meier, J. *Solid Oxide Fuel Cells V*; Stimming, Singhal, Tagawa, Lehnert, Eds.; Electrochem. Soc., Proc. Vol. 97-40; Electrochemical Society: Pennington, NJ, 1997; p 1190.

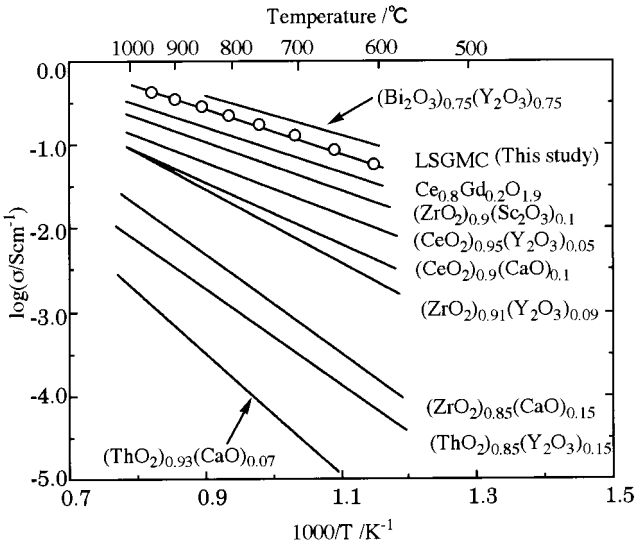

Figure 12. Comparison of oxide ion conductivity of $La_{0.8}Sr_{0.2}Ga_{0.8}Mg_{0.115}Co_{0.085}O_3$ with that of the conventional fluorite oxides.

Ga^{3+}. The mobility of the oxide ion seems to be improved by a partially substituted Co. The changes in mobility is now under investigation and the results will be published at a later date.

Comparison of the Oxide Ion Conductivity of LSGMC with That of Conventional Materials. Figure 12 shows the comparison of the oxide ion conductivity of LSGMC with that of the conventional fluorite oxides.[28] The oxide ion conductivity of LSGMC is higher than that of CeO_2 doped with Gd and slightly lower than that of the Bi_2O_3 doped with Y^{3+}. However, it is well-known that Bi_2O_3-based oxide exhibits pure oxide ion conduction within a limited range of oxygen partial pressures. In addition, the melting point of Bi_2O_3 is as low as ~1113 K and is highly reactive to form a secondary phase easily. Considering the wide oxygen partial pressure range in which oxide ion conduction is dominant, it is clear that LSGMC is a better material as a fast oxide ion conductor. Consequently, this study clearly show that LSGM doped with a small amount of Co is a promising oxide ion conducting electrolyte.

(28) Choudhary, C. B.; Maiti, H. S.; Subbarao, E. C. *Solid Electrolyte and Their Application*; Subbrao, E. C., Ed.; Plenum Press: New York, 1980; p 40.

Conclusions

The effects of doping certain transition metal cations on the oxide ion conductivity of Sr- and Mg-doped $LaGaO_3$ were investigated. It was found that Co is a promising dopant for increasing the oxide ion conductivity among the examined cations. Since the hole conduction was also increased, an excess amount of Co dopant was needed from the electrolyte point of view. Considering the ionic conductivity and transport number, the optimized composition for the Co-doped $LaGaO_3$ was $La_{0.8}Sr_{0.2}Ga_{0.8}Mg_{0.115}Co_{0.085}O_3$. The electrical conductivity of this sample was almost independent of the oxygen partial pressure from $P_{O_2} = 1$ to 10^{-21}. Consequently, Co-doped $LaGaO_3$ is also a candidate as an electrolyte for SOFCs which may be operated at lower temperatures than the current ones. The improved oxide ion conductivity by doping Co was confirmed by the ^{18}O tracer diffusion method and an oxygen permeation measurement. The mobility of the oxide ion seems to be improved by partially substituting with Co. Therefore, matching of the ionic size of the dopant with the lattice cation seems to be effective for improving the mobility of the oxide ion. Consequently, if the amount of dopant is carefully controlled, doping transition metal cations is sometimes effective for increasing the oxide ionic conductivity.

Acknowledgment. The authors acknowledge financial support from the 2nd Toyota High-tech. Research Grant Program and Nissan Research Foundation. A part of this study was financially supported by the Proposal-Based R&D Program of New Energy and Industrial Technology Development Organization (NEDO).

CM981145W